



Walter+Eliza Hall
Institute of Medical Research

Institute Research Publication Repository

This is the authors' accepted version of their manuscript accepted for publication in
Immunology & Cell Biology

The published article is available from Nature Publishing Group:

Chevrier S, Kratina T, Emslie D, Karnowski A, Corcoran LM.
Germinal center-independent, IgM-mediated autoimmunity in sanroque mice lacking
Obf1. *Immunology & Cell Biology*. 2014 Jan; 92(1):12-19. doi: [10.1038/icb.2013.71](https://doi.org/10.1038/icb.2013.71)

<http://www.nature.com/icb/journal/v92/n1/full/icb201371a.html>

Outstanding Observation

**Germinal center-independent, IgM-mediated autoimmunity in
sanroque mice lacking Obf1**

Stephane Chevrier^{1,2,5}, Tobias Kratina^{1,2,5}, Dianne Emslie^{1,2}, Alexander Karnowski³ and
Lynn M Corcoran^{1,2,4}

Running title: Autoimmunity in *sanroque/Obf1*^{-/-} mice

¹Molecular Immunology Division, The Walter and Eliza Hall Institute of Medical Research,
1G Royal Parade, Parkville, Victoria 3050, Australia

²Department of Medical Biology, The University of Melbourne, Parkville, Victoria,
Australia 3010

³CSL Limited, Bio21 Institute, 30 Flemington Road, Parkville, Victoria, Australia 3010

⁴Corresponding author

Telephone: +61-3-9345-2496

FAX: +61-3-3347-0852

email: corcoran@wehi.edu.au

⁵Contributed equally

Abstract

Mice homozygous for a point mutation in the *Rc3h1* gene encoding Roquin1, designated *sanroque* mice, develop a severe antibody-mediated autoimmune condition. The disease is T-cell intrinsic, exacerbated by macrophage-intrinsic defects, and driven by excessive T follicular helper (T_{FH}) cell generation and spontaneous germinal centre (GC) formation. This culminates in abnormally high numbers of plasma cells secreting high affinity autoreactive IgG. Obf1 is a transcriptional co-activator required for normal T cell-dependent antibody responses, and it is essential for GC formation under all circumstances so far tested. We crossed *sanroque* mice with Obf1-null mice to ask whether the hyperactivity of *sanroque* T cells could drive *Obf1*^{-/-} B cells to differentiate to GC B cells, or conversely, if Obf1 loss would prevent *sanroque*-mediated autoimmune disease. Surprisingly, while *sanroque/Obf1*^{-/-} mice did not form GC, they still developed autoimmune disease and succumbed even more rapidly than did *sanroque* mice. The disease was mediated by autoreactive IgM, which may have been derived from a pre-existing population of autoreactive B cells in the *Obf1*^{-/-} mice responding to the over-exuberant activity of *sanroque* CD4 cells.

Keywords: Autoantibody, Obf1, Sanroque

Introduction

Roquin proteins are RING-type E3 ubiquitin ligases that act as RNA binding proteins, recruiting additional factors to regulate the stability of mRNAs encoding important immune-modulating receptors and soluble factors (1-5). Mice homozygous for the hypomorphic *sanroque* (*san*) allele of the *Roquin1/Rc3h1* gene (hereafter referred to as *sanroque* mice) express a modified version of Roquin1 that leads to constitutive signalling through ICOS, an essential co-stimulatory receptor expressed most highly on follicular T helper cells (T_{FH}). As a result of this mutation, mice display splenomegaly, spontaneous T cell activation and germinal centre (GC) formation, and high levels of circulating, autoreactive antibodies of all isotypes. These autoantibodies accumulate as immune complexes in organs including the kidney, where they cause a characteristic glomerulonephritis.

The accumulation of CD4⁺ effector cells, T_{FH} cells and plasma cells is T cell intrinsic (6). Elimination of T_{FH} cells by generating *sanroque/Sh2d1a*^{-/-} double mutant mice, which lack the SAP adaptor required for T_{FH} formation, abrogates autoantibodies and kidney damage but does not ameliorate the hypercellularity and enlarged spleen or lymph nodes of mutant mice (7). Alternatively, in *sanroque* mice that lack the CD28 co-stimulatory molecule, a relative of ICOS, the accumulation of T_{FH} is unaffected, but autoantibody generation and disease frequency are reduced (7). These observations suggest that T_{FH} cell-driven GC formation and resultant high affinity IgG are central to autoimmune disease in *sanroque* mice. Roquin1 also acts in macrophages to repress the production of TNF and to attenuate autoantibody-mediated arthritis (4). Full loss of Roquin1 protein causes some functional defects, depending on the cell lineage carrying the conditional mutation, but it does not mimic the autoimmune *sanroque* phenotype (8). This is, at least in part, because ablation of Roquin1 can be complemented by Roquin2, its paralogue (4, 5).

Mice lacking the transcriptional co-activator Obf1 (also known as Bob.1 or OCA-B) fail to form GC upon immunisation or infection, and make very poor T cell-dependent (TD) antibody responses (9-13). The Obf1 mutant phenotype is B cell intrinsic (13). The cause of the GC defect is still unexplained, but may in part reflect abnormal B cell receptor (BCR) signalling by *Obf1*^{-/-} B cells (12-14). Other contributors to poor TD responses are the failure of *Obf1*^{-/-} B cells to differentiate to antibody secreting cells (ASC) under T cell-dependent conditions in vitro and in vivo (10), and the incapacity of activated Obf-1-null B cells to secrete IL6, a factor that facilitates T_{FH} induction (9, 15).

We reasoned that, as pathology in *sanroque* mice is strongly associated with T_{FH} cell generation and subsequent GC formation, mice unable to form GCs might not succumb to *sanroque*-mediated autoimmune disease. This is strongly predicted, as Linterman et al. (2007) show that loss of even one allele of Bcl6, an essential regulator of GC formation, from *sanroque* mice substantially reduces GC formation and disease prevalence in a B cell intrinsic manner (7). We therefore crossed *sanroque* mice to *Obf1* mutant mice to discover whether Obf1, like Bcl6, is required for the process that drives the over-exuberant GC response of *sanroque* mice.

Results

Loss of Obf1, and so germinal centre capacity, from Sanroque mice does not extend survival

We crossed *sanroque* mice to *Obf1* mutant mice (both on a C57BL/6 background) and generated progeny of all possible genotypes, including wild type, simple and compound heterozygotes, and single and double mutants. The health of the mice was monitored for 250 days, well beyond the typical time of onset disease in *sanroque* mice (~7 weeks for females, 8-16 weeks for males (6)).

At the time animals were euthanized (at 250 days of age, or earlier if they became ill), mice homozygous for both *san* and *Obf1* null alleles still lacked GC histologically (Figure 1a) and by cell phenotype (Figure 1b). Interestingly, spleens from diseased *sanroque/Obf1*-null mice also did not display the expanded T_{FH} cell population that is typical of diseased *sanroque* mice (Figure 1c). Surprisingly, we found that, rather than ameliorate disease, the loss of functional alleles of *Obf1* accelerated slightly the disease of mice bearing *Rc3h1^{san}* alleles (Figure 1d). Double *sanroque/Obf1^{-/-}* mutants developed disease ~60 days earlier than *sanroque/Obf1^{+/+}* mice (mean disease latency 159 days and 98 days, respectively). *Sanroque* mice heterozygous for *Obf1* had an intermediate disease latency of 116 days. Ellyard et al. (16) reported that mice heterozygous for the *Rc3h1^{san}* allele commonly developed T cell lymphoma-like tumours. We did not observe such tumours or significantly reduced viability in *Rc3h1^{san/+}* mice (Figure 1d), possibly because of differences in genetic backgrounds of the mice in the two studies (C57BL/6 here and CBAxB6 F1 and F2 in ref. 16).

Collectively these data indicate that *Obf1* deficiency prevents the differentiation of *sanroque* CD4 T cells into T_{FH} and the subsequent exuberant GC formation. However, the absence of *Obf1* was not sufficient to block the development of *sanroque*-mediated pathology, which occurs in this context in a GC independent way. Each mutation brings risk, with the combined effect being approximately additive in terms of disease prevalence.

***Obf1*-deficiency modifies the autoimmune profile of *sanroque* mice**

Mice suffering from *sanroque*-mediated autoimmunity display splenomegaly and high serum levels of most Ig isotypes, including IgG, IgA and significantly, IgE, a class not normally detected in serum of healthy mice (6). We measured spleen weights and steady state serum Ig levels from all mice in the cohort: both diseased mice and healthy mice that had reached 250 days of age without overt illness. As reported, mice homozygous for the *Rc3h1^{san}* mutation

had enlarged spleens (mean weight, 392 ± 58 mg, $n=7$) compared to wildtype (WT) controls (87 ± 17 mg, $n=4$; Figure 2a). *Obf1*-null mice had normally sized spleens (90 ± 7 mg, $n=12$). The *sanroque/Obf1*^{-/-} double mutant mice displayed similar splenomegaly to *sanroque* mice, despite lacking GC (Figure 1 and 2a), a finding comparable to *sanroque/Sh2d1a*^{-/-} mice that also lack T_{FH} cells and GC (but are devoid of autoimmunity). In *sanroque* mice and Roquin1 deficient mice, splenomegaly reflected increased numbers of GC B cells and plasma cells, but was accompanied by an increased proportion of many non-B cell populations (6, 8). Splenomegaly in *sanroque/Obf1* double mutant mice also reflected increases in non-B cells. Loss of *Obf1* causes a reduction in the proportion of B cells in the spleens of mice on both a WT and *sanroque* background (Figure 2b and refs 11, 12, 17).

Hyper IgM, IgG1, IgA and IgE were evident in all mice homozygous for *sanroque*, but additional loss of functional *Obf1* dramatically skewed the serum Ig profiles of the diseased mice. In *sanroque/Obf1*^{-/-} mice, serum IgG1 and IgA were not elevated above normal levels (Figure 2 d-e), and IgE, while detectable, was much reduced compared to *sanroque* mice with functional *Obf1* alleles (Figure 2f). Collectively, these observations suggest that disease in *sanroque/Obf1* double mutant mice is not mediated by high affinity, isotype switched, GC derived autoantibodies.

Obf1-deficient sanroque mice display an autoreactive IgM-mediated glomerulonephritis

Sanroque mice display high titres of autoreactive, anti-double-stranded (ds) DNA antibodies and deposition of IgG immune complexes in the kidney, causing severe glomerulonephritis. We also observed these features in *sanroque* mice when they were *Obf1* sufficient (Figure 3b, d and e). Histologically, kidneys of all diseased *sanroque/Obf1*^{+/+} and *sanroque/Obf1*^{+/-} mice displayed immune complex-mediated glomerulonephritis with inflammatory foci and some lymphoid infiltration. Immune complexes of IgG, but little IgM, were detected by

immunohistochemistry in kidneys of these mice, but not in control mice of the same age (Figure 3e). This correlated with very high titres of anti-nuclear antibodies and anti-dsDNA IgG1 in serum and with proteinuria (Figure 3b, c), as previously reported (6).

Upon loss of *Obf1*, autoreactive IgG1 and IgG immune complexes were no longer detectable in the serum or kidneys, respectively, of diseased mice. However, anti-nuclear and anti-dsDNA IgM was abundant in serum, and accumulated as IgM immune complexes in kidneys of double mutants (Figure 3a, d and e). Even *Obf1*-null mice with WT *Rc3h1* alleles showed slightly elevated to appreciable levels of dsDNA-specific IgM. Infiltration of myeloid and lymphoid cells into non-lymphoid tissues, such as lung, salivary glands, bladder and kidney, was common in double mutants. Plasma cells were present, but they were not the dominant cell type in the infiltrating populations (data not shown). Histologically, the pathology of the kidneys was similar in double mutant mice to *sanroque/Obf1^{+/+}* or *sanroque/Obf1^{+/-}* mice, and proteinuria was as pronounced in double mutants as in *sanroque* mice (Figure 3c).

Expanded population of IgM secreting B1 cells in Obf1^{-/-} mice

We wanted to explore the source of the high levels of autoreactive IgM found in *sanroque/Obf1^{-/-}* mice. *Obf1*-null mice on a WT background do have reduced levels of switched Ig isotypes in serum (Figure 2 and refs 11, 12, 17). This reflects a specific defect in T-cell dependent ASC differentiation; *Obf1^{-/-}* B cells switch isotype normally (10). So while GC-independent differentiation of IgM ASC from follicular B cells is a possible source of the autoreactive IgM in *sanroque/Obf1^{-/-}* mice, we focussed our attention on the B1 B cells of the peritoneal and pleural cavities. In normal mice, these cells contribute the majority of serum IgM in vivo, and they are genetically poised to differentiate rapidly to ASC upon stimulation (18, 19).

Both B1 and B2 populations were easily detectable in peritoneal lavages from WT and *sanroque* mice (Figure 4a, b), as has been reported (6). They could be divided into B1a and B1b cells on the basis of CD5 expression, and these proportions were also similar between WT and *sanroque* mice (Figure 4c). In contrast, *Obf1*^{-/-} mice had an expanded population of B1 cells, with primarily a B1b phenotype: B220^{int}, CD23⁻, Mac1/CD11b^{int} and CD5⁻ (Figure 4a-c and data not shown). To assay for inherent autoreactivity amongst these cells, total peritoneal B220⁺ cells were enriched from mice of each genotype and stimulated briefly in vitro (48 h, LPS). Supernatants were harvested and tested for reactivity with dsDNA by ELISA. Peritoneal B cells from *Obf1*^{-/-} mice generated significantly more anti-dsDNA IgM than WT or *sanroque* mice, while little anti-dsDNA IgG1 was secreted in any culture (Figure 4d). While these data do not specifically identify the B1 cells as the autoreactive population, they are consistent with the notion that *Obf1*-deficient mice harbour an expanded B1 lymphocyte population with intrinsic autoreactive potential.

We compared expression of the *Obf1*, *Rc3h1/Roquin1*, *Icos* and *Icosl* genes across FoB, B1 and GC B cell populations, using RNAseq data we obtained from sorted populations from normal C57BL/6 mice (Figure 4e), as a backdrop for considering the cause of the altered autoimmune phenotype of *sanroque/Obf-1* null mice. *Obf1* mRNA levels were low and similar in FoB, B2 and B1 cells and high in GC B, reflecting the reliance on *Obf1* for GC formation. *Rc3h1/Roquin1* expression was low and, as reported, ubiquitous across these populations. Interestingly, *Icos* expression was the inverse of *Obf1*; higher in FoB and B1 cells than GC B cells, where it was barely detectable. *Icos* and *Rc3h1/Roquin1* are co-expressed in B cells, particularly in B cells of the peritoneal cavity. Furthermore, *Obf1*^{-/-} B cells express normal levels of, *Rc3h1/Roquin1*, *Icos* and *Icosl* (RNAseq data not shown).

Discussion

Of the potential mechanistic explanations for the novel autoimmune phenotype of the double mutant mice described here, we favour models where autoreactive antibody production is driven by a *sanroque* effect on CD4 T_H cell function, and an *Obf1* mutation-mediated defect in B cell function. This is because the strongest aspects of the individual *sanroque* and *Obf1*-null phenotypes have been shown to be T cell- and B cell-intrinsic, respectively (6, 13).

However, other possibilities should be considered. Wirth and colleagues (20) have shown that *Obf1* does have an influence in T cells on the balance between T_{H1} and T_{H2} responses. In *Obf1*^{-/-} mice, T_{H1} cytokines (IFN γ and IL2) were reduced, and secretion of T_{H2} cytokines increased. In another study, we found that *Obf1*^{-/-} mice infected by influenza virus did not form GC, and T_{FH} numbers were significantly reduced (9). This could reflect either a B cell-intrinsic failure to stimulate T_{FH} formation or a T cell-intrinsic influence of *Obf1* loss. Similarly, both the null and *sanroque* alleles of *R3ch1* have some cell intrinsic impact on B cell behaviour, including a mild but statistically significant effect on GC B cell accumulation that might reflect increased B cell activation (6, 8). Finally, *Rc3h1/Roquin1* is a ubiquitously expressed RNA regulator (1, 6), which influences many RNAs in cell types besides T_{FH} (3, 8), promoting both cell intrinsic and cell extrinsic responses.

In *Obf1*-null mice, Fo B cells exhibit BCR signalling defects (14), and they lack the capacity to participate in the GC reaction that would enable affinity maturation. *Obf1*-deficient B cells are able to switch isotype normally, but display a differentiation defect in the face of T cell signals in vitro and in vivo (10). MZ B cells are absent (21), while the B1 (B1b) population is expanded. Thus, non-GC FoB and/or B1 cells must be the source of the autoreactive antibodies detected here in *sanroque/Obf1*^{-/-} mice. B1 cells, by their nature, are autoreactive. This reactivity to self is considered a side effect of the low affinity and broadly cross reactive antigen specificity of the B1 B cell pool, whose major function is to act as a pre-formed first line defence against a broad range of bacterial pathogens (18). Recruitment

into the B1 cell compartment is dependent upon antigen specificity and antigen receptor signal strength. The expansion of the B1 compartment in *Obf1*-null mice may reflect the developmental abnormalities that have been described for B lineage cells in these mice, including defects in transitional B cell selection and in the expression and rearrangement of a subset of *Igk* genes, thus skewing the repertoire (22, 23). Indeed, in the latter studies, anti-dsDNA was detected in the serum of *Obf1* mutant mice, but the cellular source was not determined and B1 cells were not examined.

Vinuesa et al. (2005) reported that *sanroque* mice that are *Obf1*-sufficient express abnormally high levels of IgM in serum (see also Figure 2c), although it was not determined whether this IgM was autoreactive or pathogenic. Data in Figure 3a here indicate that there is autoreactive IgM in *sanroque* mice. Whether this IgM is derived from abnormally activated, unswitched FoB cells in aberrant GC, or from activated B1 cells is not known. It is possible that B1 cell-derived auto-IgM contributes to autoimmunity in *sanroque* mice, and the expansion of the B1 population mediated by *Obf1* loss may accelerate this to a pathogenic level.

Taking these facts into consideration, we propose the following as possible explanations of *sanroque/Obf1* autoimmune disease:

1. An expanded and autoreactive B cell compartment of *Obf1* mice is hyperactive in the presence of factors *secreted* by *sanroque* T cells, causing expansion and/or enhanced differentiation to ASC secreting autoreactive IgM. This IgM, while likely to be of low affinity, would be able to strongly activate and fix complement at the site of tissue deposition. Whether the Fo or B1 B cell compartment of *Obf1*^{-/-} mice harbours autoreactive clones, each might be stimulated to expand or differentiate abnormally in *sanroque* mice. *Sanroque* T_{FH} cells have an activated phenotype, and overexpress a number of T cell cytokines including IL5 and IL21, which can be detected in serum (6). Regardless of the cause of B1 cell

expansion in *Obf1*-null mice, once generated, B1 cells are particularly responsive to the growth enhancing effects of IL5, as they express the high affinity IL5 receptor, CD125/IL5R α , constitutively (24). IL5 and IL21 are also both ASC differentiation factors (25-27). Under this scenario, IL5 or IL21 from *sanroque* CD4 cells could promote the expansion and differentiation of a pre-existing population of autoreactive *Obf1*^{-/-} B cells, without the need for co-localisation in a GC structure. Pratama et al., (2013) also recently reported a myeloid-cell-intrinsic effect mediated by macrophage-derived TNF (4). The same mechanism is likely to be active in *sanroque/Obf1*^{-/-} mice, but is unlikely to be exacerbated by loss of *Obf1*, as *Obf1* is not expressed in myeloid cells (28).

2. The autoreactivity of FoB/B1 cells in *Obf1*-null mice is exacerbated by *contact* with *sanroque* T cells. Clearly, the double mutant mice lack GC, the classical structures enabling the interaction of cognate B and T_{FH} cells. However, FoB cells circulate continually, and in other studies, both B1 cells and cells with a T_{FH} phenotype have been shown to circulate under activating or pathological circumstances. Simpson et al. (29) have shown that circulating T_{FH}-like cells are a marker of severe disease in lupus patients, correlating with high levels of autoantibodies. They also showed that *sanroque* mice have circulating T_{FH}-like cells in blood in proportion to their expansion in GC. B1 cells, while characteristically found most abundantly in the peritoneal and pleural cavities, and as a small minority of splenic B cells, do circulate upon mitogenic or antigenic challenge or in autoimmune conditions, and can activate peripheral CD4⁺ T cells either in the periphery or within in peritoneal cavity (30, 31). Thus autoreactive Fo/B1 cells in *Obf1*^{-/-} mice might encounter hyperactive *sanroque* CD4⁺ T cells outside of GC, and receive the necessary differentiation signals to become ASC secreting pathogenic autoantibodies. While such an encounter between B and T cells with appropriate specificities is highly unlikely in normal circumstances, the expansion of cross

reactive *Obf1*^{-/-} B cells, and polyclonal activation of *sanroque* CD4⁺ T cells may increase the probability.

3. Alternatively to models 1 and 2 above, which enlist B cell:T cell cooperation in the aetiology of disease in *sanroque/Obf1* null mice, in this model the effect is B cell intrinsic (and both GC and T cell independent), due to a combined effect of the *Obf1* and *sanroque* mutations in B cells. As no GC B cells are present in the double mutant, FoB or more likely, the B1 B cell compartment is the source of the autoreactive IgM. *Obf1*, *Rc3h1/Roquin1* and *Icos* are all expressed in FoB and B1 cells, but *Icosl* is not expressed in B1 cells. Thus the *sanroque* effect on Icos signalling could not act in an autocrine manner on B1 cells.

These studies have highlighted an interesting case of antibody-mediated autoimmune disease in the absence of high affinity IgG. Distinguishing between these models would require the generation of mixed chimeras where the *sanroque* and *Obf1* mutations were confined to only the B cell or the T cell lineage, and additional chimeras where double mutant B or T cells developed alongside WT cells. Interestingly, the phenotype of *sanroque/Obf1*^{-/-} mice contrasts with that reported for *sanroque/Bcl6*^{+/-} mice (7). Both display reduced GC formation, but in the former case, autoimmunity still occurs, while in the latter, it is diminished. This highlights a distinction between *Obf1* and *Bcl6* as essential intrinsic regulators of GC formation and antibody responses.

Studies using *sanroque* mice carrying mutations in other genes (*Bcl6*, *Sh2d1a/SAP*, *CD28*) point to the importance of GC expansion in this model of autoimmune disease (7). However, it is not simply the expansion of the T_{FH} compartment, but the capacity for these hyperactive CD4 cells to provoke a response from inappropriately selected, and so autoreactive B cells. In *sanroque* mice, the CD4 cells are likely the source of this inappropriate selection (in the form of excessive T_{FH} help in a GC). In *sanroque/Obf1*^{-/-} mice,

the inappropriate selection may reflect a developmental and B cell intrinsic defect, preceding the involvement of GC.

Materials and Methods

Mice and immunisation

San^{+/+} mice were generously provided by Prof Carola Vinuesa. These were mated with *Obf1*^{-/-} mice (11) to generate double mutant mice. To induce an immune response, mice were injected i.p. with 2×10^8 sheep red blood cells (Applied Biological Products Management Ltd) or NP-KLH, as described (10). All mice were maintained on a C57BL/6 background at the specific pathogen-free facilities of The Walter and Eliza Hall Institute, and experiments were undertaken according to Animal Ethics Committee guidelines and approval.

Antibodies

For flow cytometry, histology or immunohistochemistry, the following antibodies were used: anti-B220 (clone RA3-6B20), anti-CD11b/Mac1 (M1/70), anti-CD23 (B3B4), anti-CD5 (53-7.3), anti-CD95/Fas (Jo2), anti-CXCR5 (2G8), all from BD Biosciences; anti-CD3 (SP7) was from Thermo Scientific; anti-GL7 was from eBioscience; anti-PD1 (RMP1-30) was from BioLegend. For flow cytometry, propidium iodide was included to identify dead cells, which were excluded from the analyses.

ELISA

Enzyme linked immunosorbent assays (ELISAs) were performed on mouse serum as described previously (9). Anti-dsDNA assays were performed using a Quanta Lite dsDNA ELISA kit from INOVA Diagnostics, according to the manufacturer's protocol, except that anti-mouse IgM and IgG1 HRP-conjugated secondary antibodies (Southern Biotech) were

used in place of the anti-human Ig secondary provided with the kit. All sera were assayed at a 1/300 dilution (Figure 3), and culture supernatants (Figure 4) were analysed at a standard dilution of 1 in 2.

Immunohistochemistry

Immunofluorescence staining for GC was performed as described in (9). Anti-nuclear antibodies were detected using a Hep-2 cell assay (Immunoconcepts ANA Test System) according to the manufacturer's protocol, but using anti-mouse Ig secondary reagents. Paraformaldehyde fixed kidney sections were stained with HRP-conjugated rabbit anti-mouse IgG or IgM (Soutehrn Biotech), developed and counterstained with haematoxylin. Proteinuria was determined using Multistix 10SG Reagent strips for Urinalysis (Siemens Healthcare Diagnostics).

In vitro culture

Anti-B220 magnetic beads (Miltenyi) were used to purify B cells from peritoneal lavages, and purity was typically at least 95%. Purified cells were cultured at 10^6 cells per ml in 100 μ l for 48 h and stimulated with 10 μ g/ml lipopolysaccharide (LPS, Sigma) in DME supplemented with 10% FCS, 2mM L-Glutamine, 0.1mM L-Asparagine, non-essential amino acids (Sigma) and 50 μ M 2-mercaptoethanol. Supernatants were harvested and assessed for dsDNA reactivity as described above.

Acknowledgements

We are indebted to Prof Carola Vinuesa for Sanroque mice and for many helpful comments during this work and on the manuscript. We are also extremely grateful to Prof Donald Metcalf for histology and pathology, to Dr Lachlan Whitehead for help with

immunofluorescence, to Kathy D'Costa for technical assistance and to Louise Inglis for animal husbandry. This work was made possible through Victorian State Government Operational Infrastructure Support and Australian Government NHMRC IRIS and research grants from the NHMRC (#637306 and #575500).

References

1. Athanasopoulos V, Barker A, Yu D, Tan AH, Srivastava M, Contreras N, et al. The ROQUIN family of proteins localizes to stress granules via the ROQ domain and binds target mRNAs. *The FEBS journal*. 2010 May;277(9):2109-27. PubMed PMID: 20412057.
2. Glasmacher E, Hoefig KP, Vogel KU, Rath N, Du L, Wolf C, et al. Roquin binds inducible costimulator mRNA and effectors of mRNA decay to induce microRNA-independent post-transcriptional repression. *Nat Immunol*. 2010 Aug;11(8):725-33. PubMed PMID: 20639877.
3. Leppek K, Schott J, Reitter S, Poetz F, Hammond MC, Stoecklin G. Roquin promotes constitutive mRNA decay via a conserved class of stem-loop recognition motifs. *Cell*. 2013 May 9;153(4):869-81. PubMed PMID: 23663784.
4. Pratama A, Ramiscal RR, Silva DG, Das SK, Athanasopoulos V, Fitch J, et al. Roquin-2 shares functions with its paralog Roquin-1 in the repression of mRNAs controlling T follicular helper cells and systemic inflammation. *Immunity*. 2013 Apr 18;38(4):669-80. PubMed PMID: 23583642.
5. Vogel KU, Edelmann SL, Jeltsch KM, Bertossi A, Heger K, Heinz GA, et al. Roquin paralogs 1 and 2 redundantly repress the Icos and Ox40 costimulator mRNAs and control follicular helper T cell differentiation. *Immunity*. 2013 Apr 18;38(4):655-68. PubMed PMID: 23583643.
6. Vinuesa CG, Cook MC, Angelucci C, Athanasopoulos V, Rui L, Hill KM, et al. A RING-type ubiquitin ligase family member required to repress follicular helper T cells and autoimmunity. *Nature*. 2005 May 26;435(7041):452-8. PubMed PMID: 15917799.
7. Linterman MA, Rigby RJ, Wong RK, Yu D, Brink R, Cannons JL, et al. Follicular helper T cells are required for systemic autoimmunity. *J Exp Med*. 2009 Mar 16;206(3):561-76. PubMed PMID: 19221396. Pubmed Central PMCID: 2699132.
8. Bertossi A, Aichinger M, Sansonetti P, Lech M, Neff F, Pal M, et al. Loss of Roquin induces early death and immune deregulation but not autoimmunity. *J Exp Med*. 2011 Aug 29;208(9):1749-56. PubMed PMID: 21844204. Pubmed Central PMCID: 3171092.
9. Karnowski A, Chevrier S, Belz GT, Mount A, Emslie D, D'Costa K, et al. B and T cells collaborate in antiviral responses via IL-6, IL-21, and transcriptional activator and coactivator, Oct2 and OBF-1. *J Exp Med*. 2012 Oct 22;209(11):2049-64. PubMed PMID: 23045607. Pubmed Central PMCID: 3478936.
10. Corcoran LM, Hasbold J, Dietrich W, Hawkins E, Kallies A, Nutt SL, et al. Differential requirement for OBF-1 during antibody-secreting cell differentiation. *J Exp Med*. 2005 May 2;201(9):1385-96. PubMed PMID: 15867091.
11. Schubart DB, Rolink A, Kosco-Vilbois MH, Botteri F, Matthias P. B-cell-specific coactivator OBF-1/OCA-B/Bob1 required for immune response and germinal centre formation. *Nature*. 1996;383(6600):538-42. PubMed PMID: 8849727.
12. Kim U, Qin XF, Gong S, Stevens S, Luo Y, Nussenzweig M, et al. The B-cell-specific transcription coactivator OCA-B/OBF-1/Bob-1 is essential for normal production of immunoglobulin isotypes. *Nature*. 1996;383(6600):542-7. PubMed PMID: 8849728.
13. Qin XF, Reichlin A, Luo Y, Roeder RG, Nussenzweig MC. OCA-B integrates B cell antigen receptor-, CD40L- and IL 4-mediated signals for the germinal center pathway of B cell development. *Embo J*. 1998;17(17):5066-75. PubMed PMID: 9724642.
14. Brunner C, Marinkovic D, Klein J, Samardzic T, Nitschke L, Wirth T. B cell-specific transgenic expression of Bcl2 rescues early B lymphopoiesis but not B cell responses in BOB.1/OBF.1-deficient mice. *J Exp Med*. 2003 May 5;197(9):1205-11. PubMed PMID: 12732662. Pubmed Central PMCID: 2193979.

15. Dienz O, Eaton SM, Bond JP, Neveu W, Moquin D, Noubade R, et al. The induction of antibody production by IL-6 is indirectly mediated by IL-21 produced by CD4+ T cells. *J Exp Med*. 2009 Jan 16;206(1):69-78. PubMed PMID: 19139170. Pubmed Central PMCID: 2626667.
16. Ellyard JI, Chia T, Rodriguez-Pinilla SM, Martin JL, Hu X, Navarro-Gonzalez M, et al. Heterozygosity for Roquinsan leads to angioimmunoblastic T-cell lymphoma-like tumors in mice. *Blood*. 2012 Jul 26;120(4):812-21. PubMed PMID: 22700722.
17. Nielsen PJ, Georgiev O, Lorenz B, Schaffner W. B lymphocytes are impaired in mice lacking the transcriptional co-activator Bob1/OCA-B/OBF1. *Eur J Immunol*. 1996;26(12):3214-8. PubMed PMID: 8977324.
18. Hayakawa K, Hardy RR. Development and function of B-1 cells. *Curr Opin Immunol*. 2000 Jun;12(3):346-53. PubMed PMID: 10858035.
19. Fairfax KA, Corcoran LM, Pridans C, Huntington ND, Kallies A, Nutt SL, et al. Different kinetics of blimp-1 induction in B cell subsets revealed by reporter gene. *J Immunol*. 2007 Apr 1;178(7):4104-11. PubMed PMID: 17371965. eng.
20. Brunner C, Sindrilaru A, Girkontaite I, Fischer KD, Sunderkotter C, Wirth T. BOB.1/OBF.1 controls the balance of TH1 and TH2 immune responses. *EMBO J*. 2007 Jul 11;26(13):3191-202. PubMed PMID: 17568779. Pubmed Central PMCID: 1914090.
21. Samardzic T, Marinkovic D, Nielsen PJ, Nitschke L, Wirth T. BOB.1/OBF.1 deficiency affects marginal-zone B-cell compartment. *Mol Cell Biol*. 2002 Dec;22(23):8320-31. PubMed PMID: 12417733.
22. Casellas R, Jankovic M, Meyer G, Gazumyan A, Luo Y, Roeder R, et al. OcaB is required for normal transcription and V(D)J recombination of a subset of immunoglobulin kappa genes. *Cell*. 2002 Sep 6;110(5):575-85. PubMed PMID: 12230975.
23. Jankovic M, Nussenzweig MC. OcaB regulates transitional B cell selection. *Int Immunol*. 2003 Sep;15(9):1099-104. PubMed PMID: 12917262.
24. Hitoshi Y, Yamaguchi N, Mita S, Sonoda E, Takaki S, Tominaga A, et al. Distribution of IL-5 receptor-positive B cells. Expression of IL-5 receptor on Ly-1(CD5)+ B cells. *J Immunol*. 1990 Jun 1;144(11):4218-25. PubMed PMID: 1692859. eng.
25. Hasbold J, Corcoran LM, Tarlinton DM, Tangye SG, Hodgkin PD. Evidence from the generation of immunoglobulin G-secreting cells that stochastic mechanisms regulate lymphocyte differentiation. *Nat Immunol*. 2004 Jan;5(1):55-63. PubMed PMID: 14647274.
27. Kuchen S, Robbins R, Sims GP, Sheng C, Phillips TM, Lipsky PE, et al. Essential role of IL-21 in B cell activation, expansion, and plasma cell generation during CD4+ T cell-B cell collaboration. *J Immunol*. 2007 Nov 1;179(9):5886-96. PubMed PMID: 17947662.
28. Zhou L, Nazarian AA, Xu J, Tantin D, Corcoran LM, Smale ST. An inducible enhancer required for Il12b promoter activity in an insulated chromatin environment. *Mol Cell Biol*. 2007 Apr;27(7):2698-712. PubMed PMID: 17242186. Pubmed Central PMCID: 1899891.
29. Simpson N, Gatenby PA, Wilson A, Malik S, Fulcher DA, Tangye SG, et al. Expansion of circulating T cells resembling follicular helper T cells is a fixed phenotype that identifies a subset of severe systemic lupus erythematosus. *Arthritis Rheum*. 2010 Jan;62(1):234-44. PubMed PMID: 20039395.
30. Margry B, Wieland WH, van Kooten PJ, van Eden W, Broere F. Peritoneal cavity B-1a cells promote peripheral CD4 T-cell activation. *Eur J Immunol*. 2013 May 30. PubMed PMID: 23719868.
31. Yan J, Mamula MJ. B and T cell tolerance and autoimmunity in autoantibody transgenic mice. *Int Immunol*. 2002 Aug;14(8):963-71. PubMed PMID: 12147633.

Figure legends

Figure 1. Survival and germinal centre cells in mice with *Obf1* and *Rc3h1^{san}* mutations

(a) Representative immunohistochemistry on spleens of diseased mice of the indicated genotypes, stained for B cells (B220), GC (GL7) and T cells CD3. (b) Percentage of splenic B220⁺ cells displaying a GC phenotype (CD95/Fas⁺, GL7⁺) in spleens of diseased mice, or healthy mice taken at 250 days of age. Each symbol represents an individual animal. Open bars represent WT mice analysed 7 days after immunisation with NP-KLH. (c) Percentage of splenic CD4⁺ cells displaying a T_{FH} phenotype (PD1⁺, CXCR5⁺) in spleens of diseased mice, or healthy mice taken at 250 days of age. Open bars represent WT mice analysed 7 days after immunisation with NP-KLH. (d) Kaplan-Meier survival curve for mice of the indicated genotypes. The numbers of mice analysed for each genotype are: *Rc3h1^{+/+}Obf1^{+/+}* (n=4); *Rc3h1^{+/+}Obf1^{-/+}* (n=27); *Rc3h1^{+/+}Obf1^{-/-}* (n=61); *Rc3h1^{san/+}Obf1^{+/+}* (n=21); *Rc3h1^{san/+}Obf1^{-/+}* (n=44); *Rc3h1^{san/+}Obf1^{-/-}* (n=48); *Rc3h1^{san/san}Obf1^{+/+}* (n=9); *Rc3h1^{san/san}Obf1^{-/+}* (n=35); *Rc3h1^{san/san}Obf1^{-/-}* (n=27).

Figure 2. Spleen weights and serum antibody levels in mice with *Obf1* and *Rc3h1^{san}* mutations

(a) Spleen weights of diseased animals, or healthy mice taken at 250 days of age, according to genotype. (b) Average percentage of live splenocytes that were B220⁺ in mice of each genotype at the time of sacrifice (when ill, or at 250 days if healthy). (c-f) Serum immunoglobulin levels in animals of the indicated genotypes at the time of sacrifice, or at 250 days. Each symbol represents an independent mouse. Means and SD are shown.

Figure 3. Evidence of autoimmunity in mice with *Obf1* and *Rc3h1^{san}* mutations

(a) Anti-dsDNA IgM levels in serum from mice of the indicated genotypes, as determined by ELISA. (b) Anti-dsDNA IgG1 levels in serum from mice of the indicated genotypes, as determined by ELISA. Means and SD are shown. (c) Proteinuria as determined in Materials and Methods in mice at the time of sacrifice. For *sanroque* mice, n=22; for *sanroque/Obf1^{-/-}* mice, n = 20. All 6 WT mice tested had urine protein levels below 30 mg/dl. (d) Hep-2 cell assay for anti-nuclear reactivity in serum from mice of the genotypes shown. Representative results using sera from three independent mice of each genotype are shown. Sera from WT B6 mice were negative in this assay. (e) Kidney immunohistochemistry to detect immune complexes, using anti-IgG- or IgM-specific primary antibodies. Images are representative of four mice for each genotype.

Figure 4. *Obf1^{-/-}* mice have an expanded peritoneal B1b cell compartment

(a) Flow cytometric staining of peritoneal lavage cells from healthy, naïve C57BL/6, *sanroque* and *Obf1^{-/-}* mice, stained to identify B1a and B1b cell populations. Top panels are gated on live cells, the bottom panels, on live, B220⁺ cells. (b) Average percentage of B1 cells in the peritoneal B cell population. Values are means ± SD (n=3 mice per group). (c) Average representation of B2, B1a and B1b lymphocytes among the B220⁺ cell pools of peritoneal cells from mice of the indicated genotypes. Values are means ± SD (n=3-6 mice per group). (d) Anti-dsDNA IgM and IgG1 levels in culture supernatants of LPS activated peritoneal B cells, as determined by ELISA. Values are means ± SD (n=3-4 mice per group). (e) RNAseq data expressed as normalised RPKM (reads per kilobase per million) for a selection of sorted C57BL/6 mouse B cell populations: FoB, small naïve follicular B cells from spleen (B220⁺, CD23⁺), Peritoneal cavity B2 and B1 cells (B220⁺, CD23⁺, Mac1⁻ and B220⁺, CD23⁻, Mac1^{lo}, respectively) and GC B cells (7 days post sheep red blood cell immunisation).

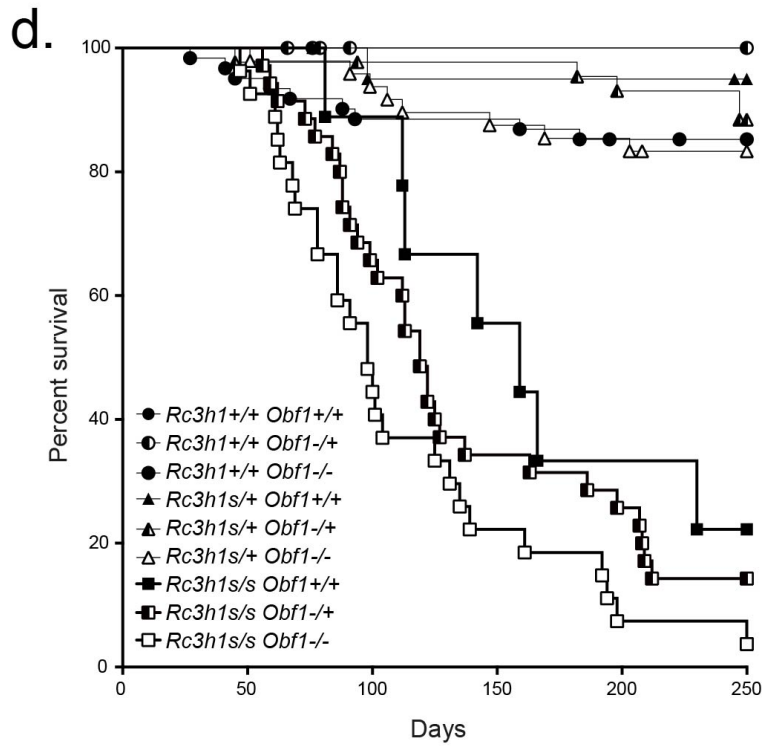
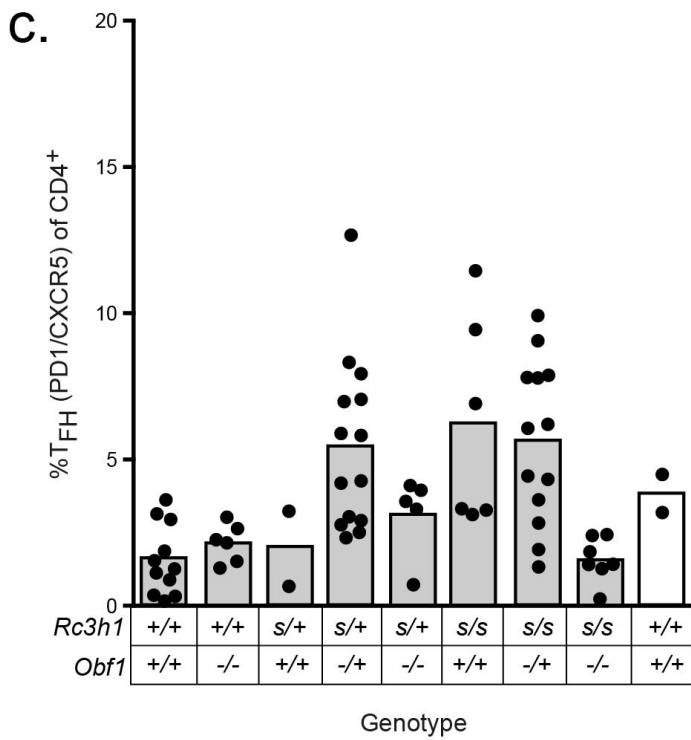
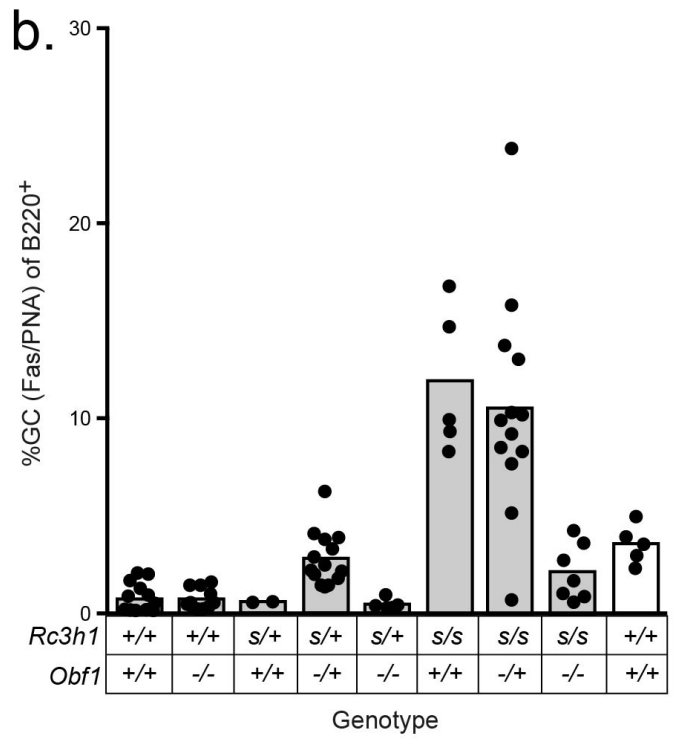
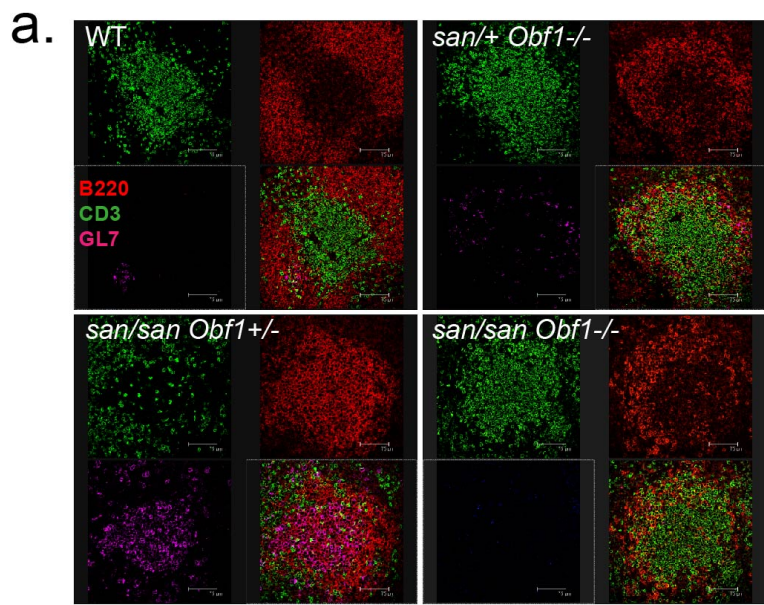


Figure 1. Chevrier et al.

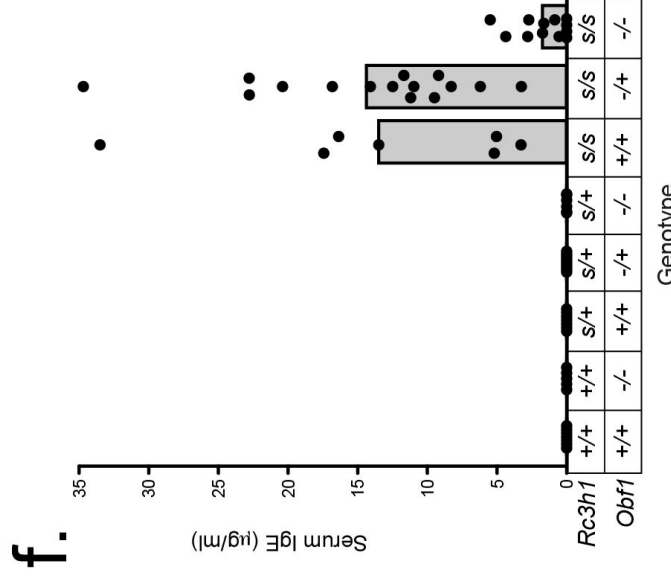
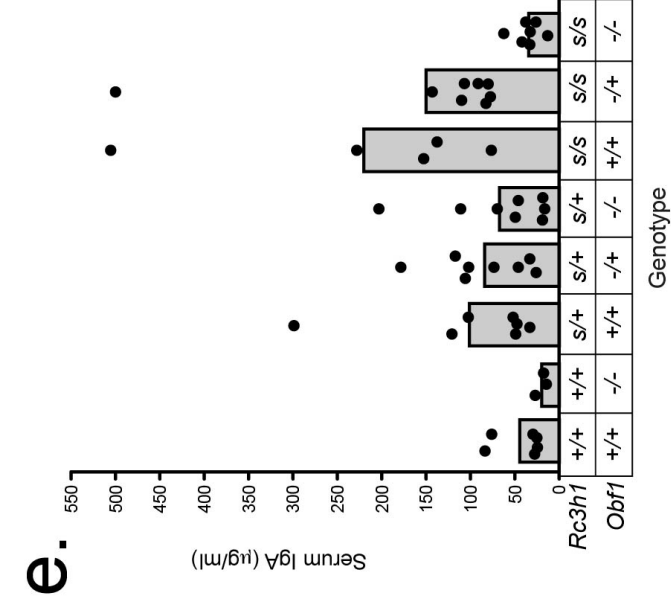
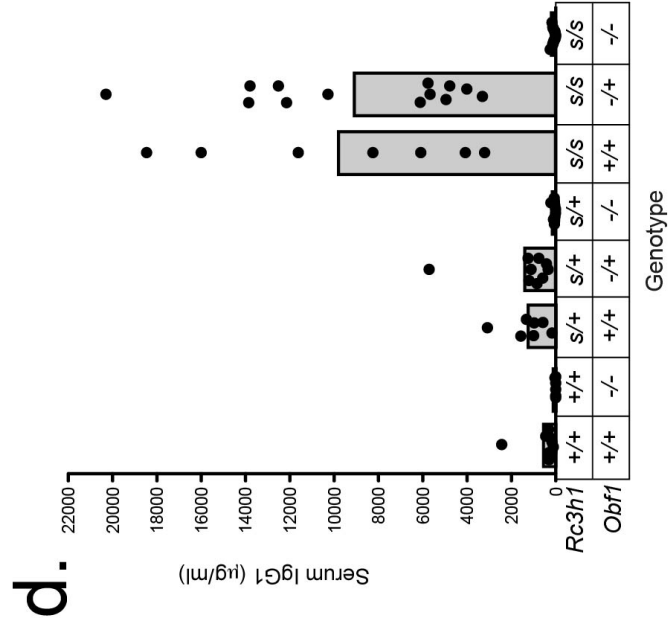
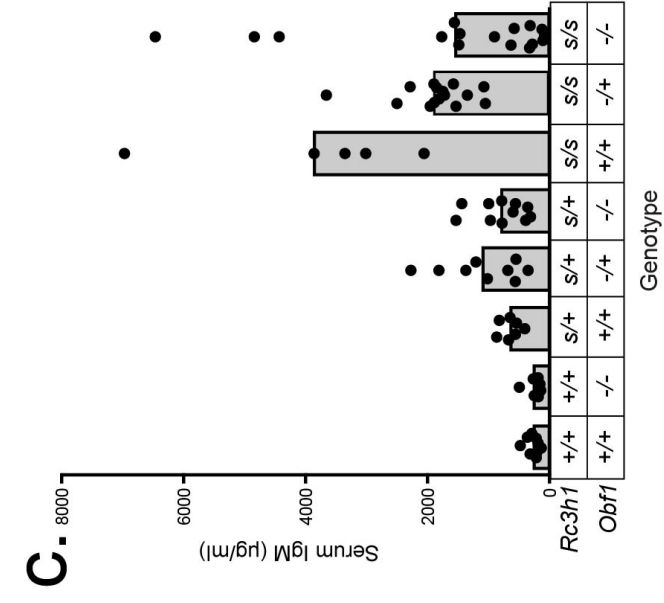
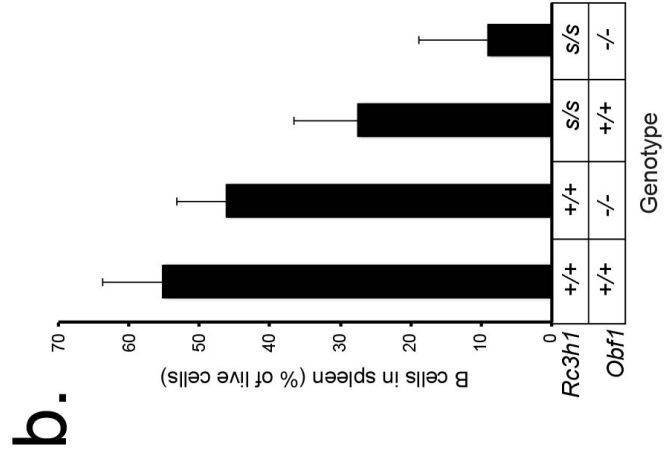
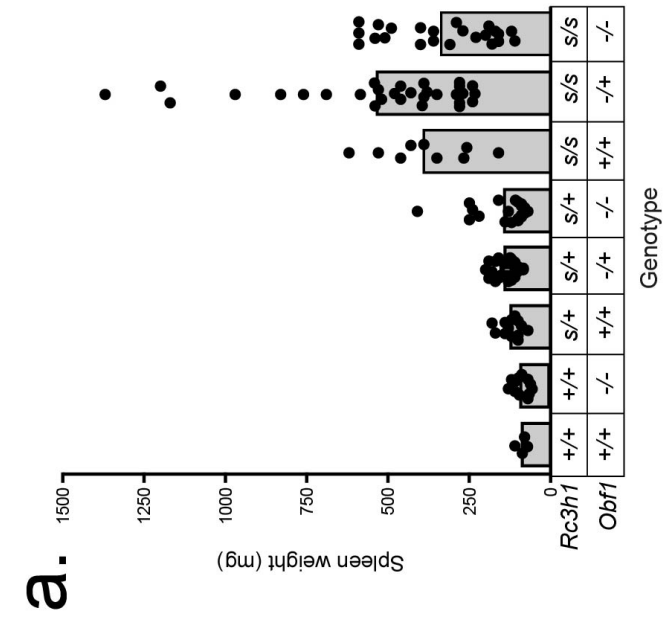


Figure 2. Chevrier et al.

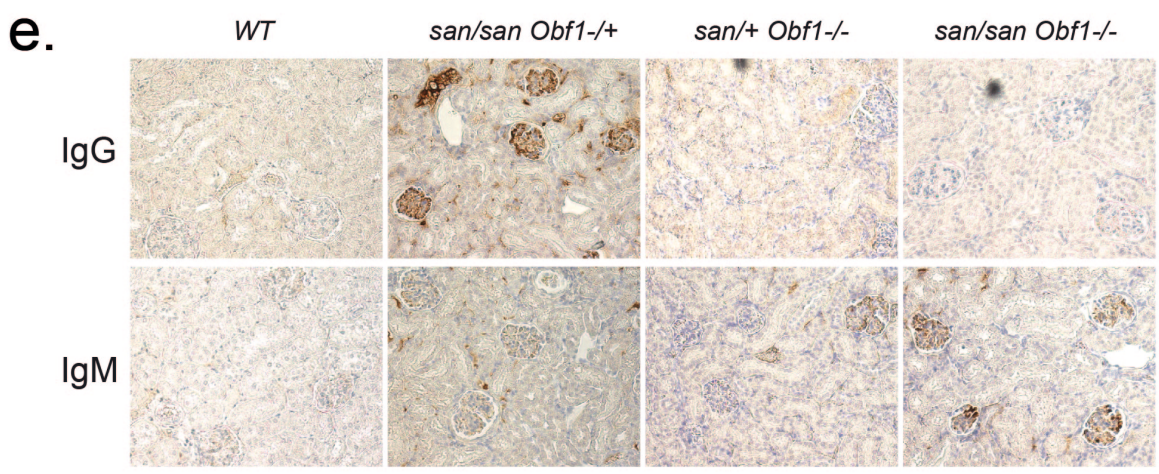
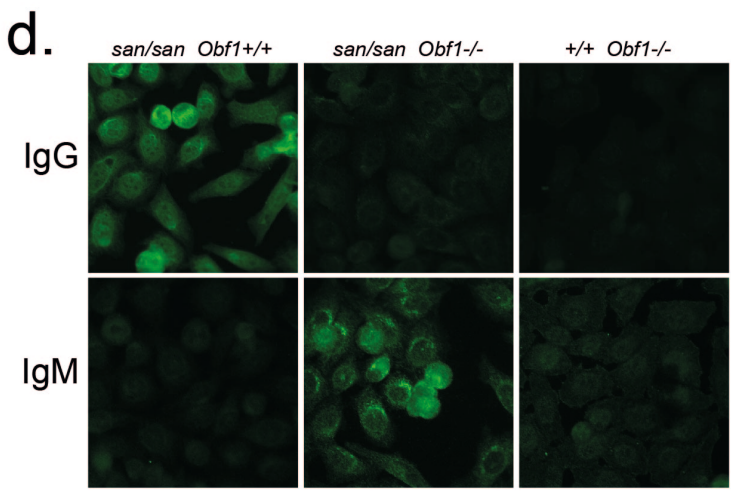
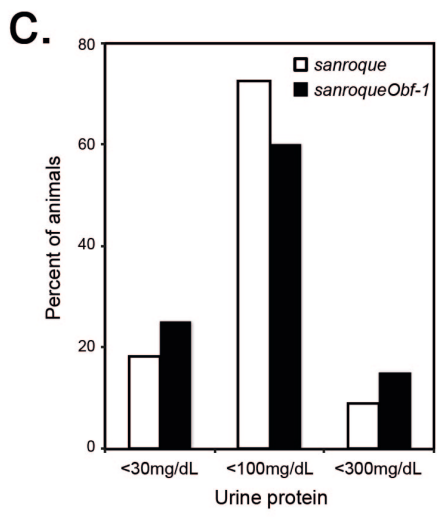
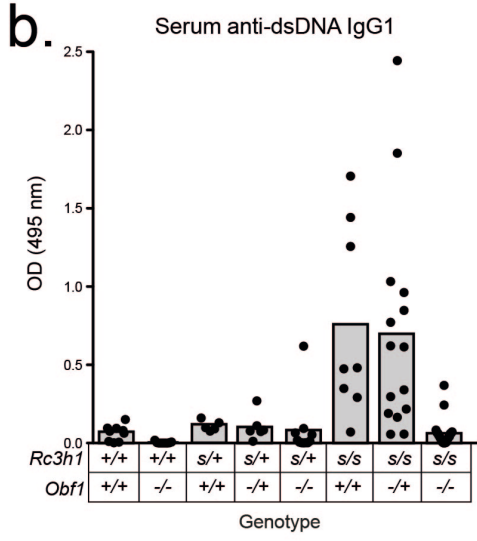
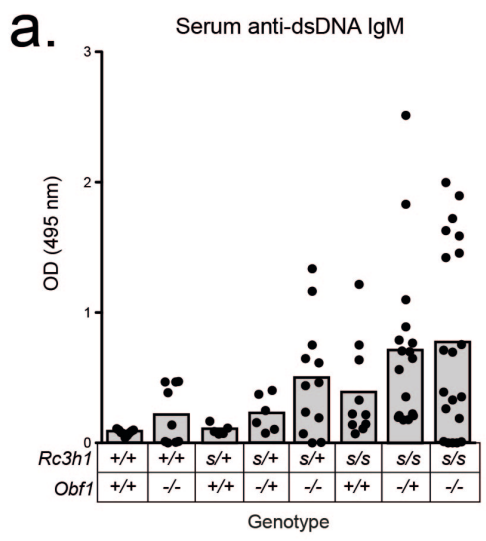


Figure 3. Chevrier et al.

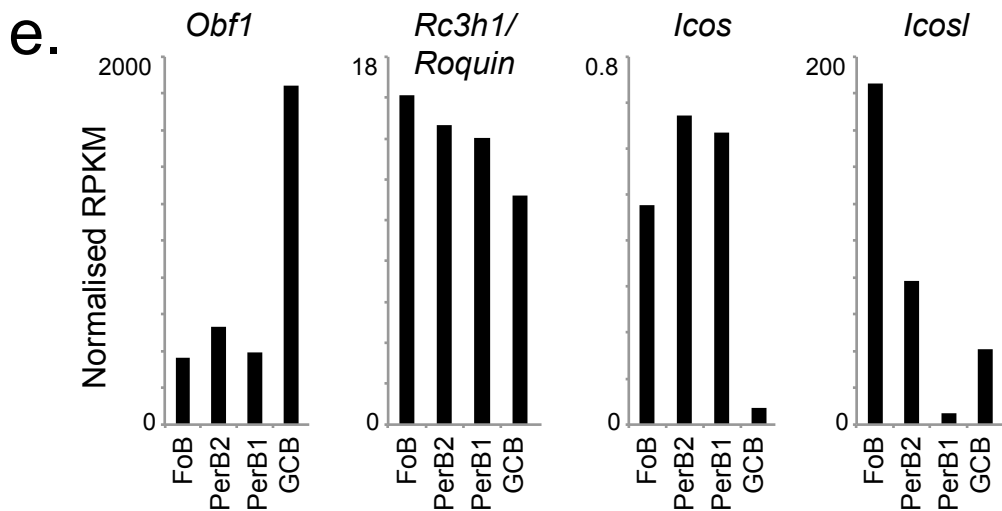
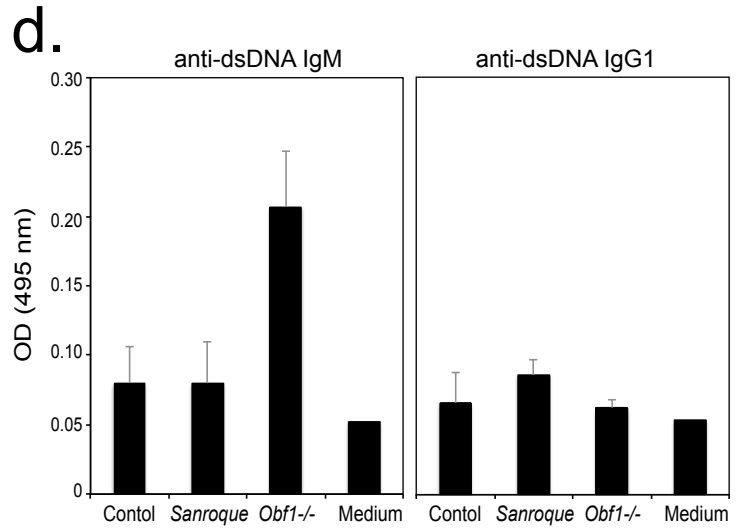
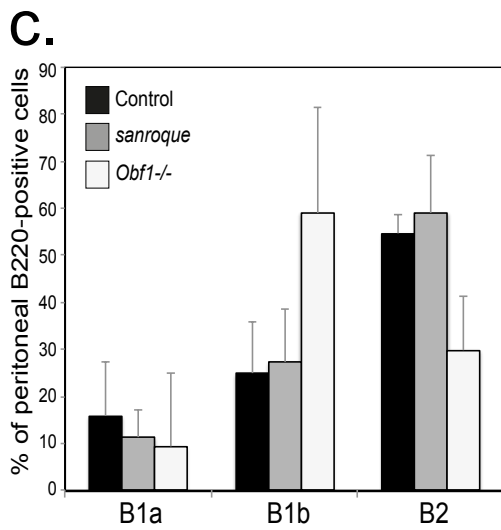
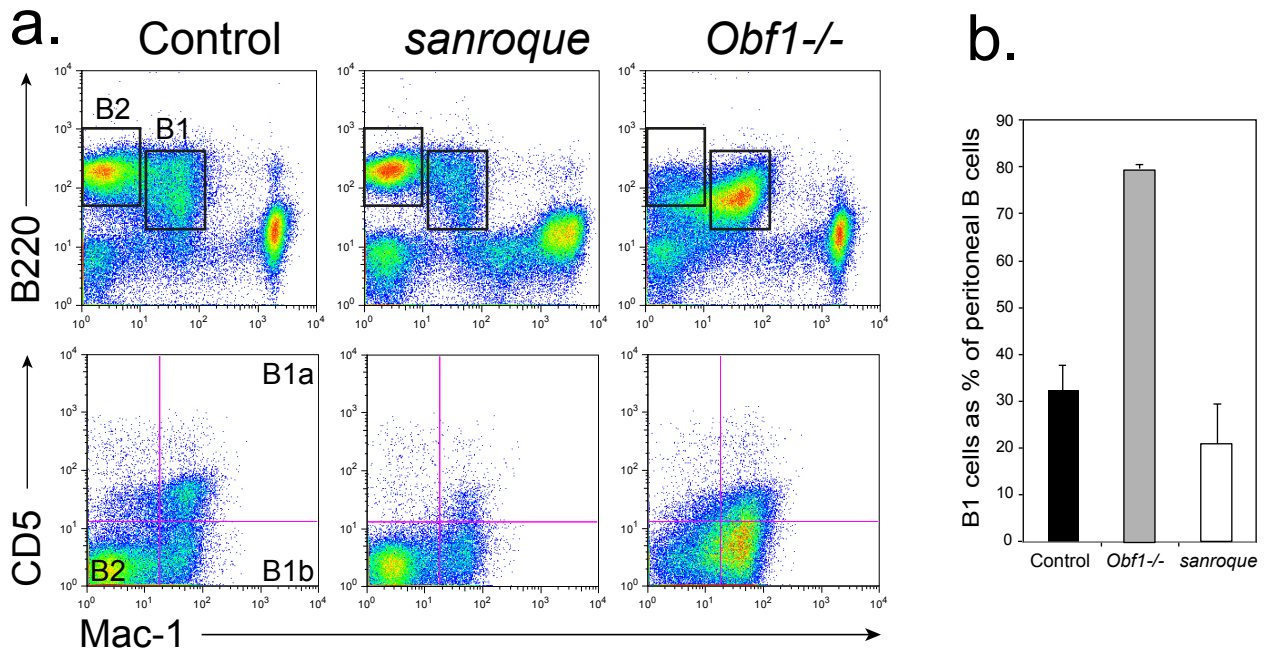


Figure 4. Chevrier et al.